JCTC Journal of Chemical Theory and Computation

Article

pubs.acs.org/JCTC

Exploring Relative Thermodynamic Stabilities of Formic Acid and Formamide Dimers – Role of Low-Frequency Hydrogen-Bond Vibrations

Michael A. Cato, Jr.,[†] D. Majumdar,*[,†] Szczepan Roszak,*[,‡] and Jerzy Leszczynski*[,†]

[†]Interdisciplinary Center for Nanotoxicity, Jackson State University, Jackson, Mississippi 39217, United States

[‡]Institute of Physical and Theoretical Chemistry, Wroclaw University of Technology, Wybrzeze Wyspianskiego 27, 50-370 Wroclaw, Poland

Supporting Information

ABSTRACT: The low-frequency fundamentals together with the high-frequency modes, responsible for hydrogen bonding (OH/NH stretching modes), were analyzed to correlate the intensities with the hydrogen-bond strengths/binding energies of the formic acid and formamide dimers using Møller–Plesset second-order perturbation (MP2) and coupled cluster computations with explicit anharmonicity corrections. Linear correlations were observed for both the formic acid and formamide dimers, and as consequence of such correlation an additive properties of binding energies with respect to the local hydrogen-bond energies of fragments involved (for these dimers) has been proposed. It has been further observed that (i) the nature of their six low-frequency fundamentals are very similar, and (ii) the in-plane bending and stretch–bend fundamentals of different dimers of these two species (depending on the dimer structure), in this low-frequency region, modulate their strength of hydrogen-bond/binding hence their relative stability order. These results were further verified against the results from Gaussian-G4-MP2 (G4MP2), Gaussian-G2-MP2 (G2MP2), and complete basis set (CBS-QB3) methods of high accuracy energy calculations.

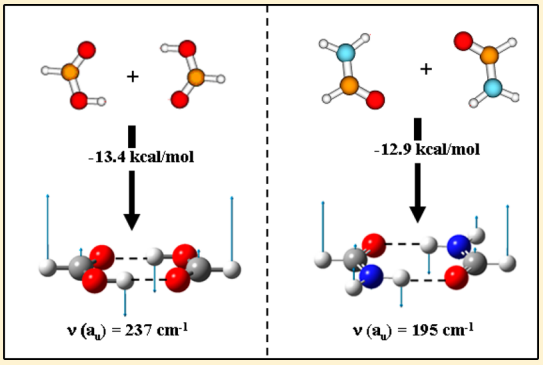

I. INTRODUCTION

Formic acid and formamide are the two smallest molecular systems known for their importance in biology. Formic acid is also one of the smallest models for rotational isomerism. It predominantly exists in *trans*-form and is well characterized through microwave studies,[1,2] electron diffraction,[3−5] infrared (IR)[6,7] and Raman[8,9] spectroscopy. The *cis*-variety is of higher energy and less abundant.[10] It could be formed through vibrational excitation of the lower-energy *trans*-conformer by narrow–band IR light.[11] The conformational behavior of formic acid has opened up a unique characteristic of this molecule – the possibility of formation of a large variety of dimeric forms. For a long time, there were speculations about such dimers through theoretical computations, and a few of them were identified experimentally.[12−14] In 2010 and onward, Marushkevich and co-workers performed a series of experiments based on vibrational excitations of ground state *trans*-formic acid and detected all the possible formic acid dimers formed through *trans*–*trans*, *trans*–*cis*, and *cis*–*cis* combinations of the monomers.[15−17] Formamide does not have the rotamerism property of formic acid, although the most abundant dimers of these two molecules are very similar.[18] Five possible dimeric forms of formamide have been predicted so far (from different orientations of the monomers) of which three have been identified experimentally through matrix isolation spectroscopy.[18,19] Thus it is important to investigate the basic structural factors, which govern the higher stability of the most abundant form of these dimers over the others.

The most abundant dimer of formic acid (*trans*–*trans*) is a six member planar ring system and was the subject of various experimental and theoretical investigations for their spectroscopic[20] and double proton transfer[21−23] properties. The assignment of various other dimers has further opened up research on their relative stabilities, their vibrational characteristics, and mechanism of their formation.[15−17] Most of these dimers have double hydrogen-bonding, although in a few cases dimers bonded through a single hydrogen-bond are possible.[12−17] The relative stabilities would mostly depend on the combinations of *trans*- and *cis*-conformers of formic acid to form such dimers, and computations of binding energies should correlate with their relative stabilities. Obviously, any dimer with *cis*-combination of formic acid monomer would be less abundant, and experimentally such isomers are formed through vibronic excitation of the *trans*-conformer.[15−17] The most abundant dimer of formamide also has a six-member ring planar structure. All of the four other possible dimers are predicted to be connected through hydrogen-bond/s with different orientation of the monomers.[18,19] The deformation of the monomer structures, affecting the strength of the hydrogen

Received: October 12, 2012
Published: January 7, 2013

bonds in various dimers, is mostly responsible for their relative stability order. Although, the formamide dimer is a model for many biological systems (e.g., in double proton transfer in nucleic acid base pairs, and peptides), only a few experimental and theoretical studies are available. These are mostly related to the assignments of such dimers based on the nature of hydrogen bonding interactions.[18,19,24]

One of the most important aspects of the formic acid and formamide dimers is the stability of the most abundant planar isomer over the others.[12−19] The computation of binding energies of these dimers and the assignment of several of their vibrational modes with respect to the experiment generally settles their relative stability order. Mostly, these approaches are oriented around the use of density functional (DFT) and Møller−Plesset second-order perturbation (MP2) theory calculations without explicit consideration of the effect of anharmonicity on binding energies and vibrational modes.[12−19] These computed results are successful in predicting the relative stability and with certain accuracy several vibrational modes (at high frequency range), albeit they scarcely generate any quantitative understanding of the origin of their relative stability order. Recent low-frequency assignments of the most abundant *trans*−*trans* formic acid dimer using jet-cooled Raman spectroscopy have probed the stiffness of the double hydrogen-bond involved in dimer formation.[25] The experiment primarily points to the importance of anharmonicity effects on the observed vibrational modes together with mode/s responsible for the stiffness of such hydrogen-bonds. The questions that naturally arise from such observations are as follows: (a) whether there is any correlation between the binding energies of such dimers and the stiffness factor (interpreted as the low frequency mode/s involving hydrogen-bond vibration) and (b) are the similarities of hydrogen bonding patterns of the most stable formic acid and formamide dimers originated from the properties of such low-frequency modes. The answers to these questions are the main objectives of our present theoretical studies. We also intend to investigate whether binding energies of such weakly bound systems could have simple additive properties based on the derived local binding energies of the constituting fragments. Such additive properties are quite natural, if the changes in the binding energies of such isomers are quite regular with respect to their structural arrangements. The predictive part of our investigation would require reliable computation of binding energies and vibrational frequencies of the various isomers of formic acid and formamide dimers.

We have computed the structure, binding energies, and vibrational characteristics of various formic acid and formamide dimers using MP2 and coupled cluster level of theories. Explicit anharmonicity corrections are taken into account to compute the binding energies, related thermodynamic quantities of binding (viz., Gibbs free energy (ΔG^{B}_{298}) and enthalpy (ΔH^{B}_{298})), and the vibrational frequencies. Six *trans*−*trans* and five *cis*−*trans* monomer combinations[15,16] have been considered for formic acid dimers, and the computed results are compared with five possible formamide dimers. We did not consider the *cis*−*cis* combinations[17] of formic acid dimers as they are known to be of very high energy and may be important to explore the complete dimer-space of formic acid. The eleven dimers considered in the present work are relatively lower in energy, and they are sufficient to substantiate our view on the relative stability order of such dimers. The low-frequency fundamentals together with their respective overtones are computed for the dimers of both formic acid and formamide. The related experimental data on the formic acid dimer[8,25] is compared with its computed lowest energy dimer, and it would be shown that the intensities of the low-frequency in-plane bending modes together with the high frequency OH/NH stretching modes of the formic acid/formamide dimers correlate linearly with their binding energies (or hydrogen-bond energies) and thus modulate the hydrogen-bond strengths (and hence relative stabilities) of these dimers. The observed correlations are further validated from the results of three high-accuracy energy calculations viz. G4MP2, G2MP2, and CBS-QB3.

II. METHODS OF COMPUTATION

The computation of the structural parameters and vibrational frequencies of the formic acid and formamide dimers were carried out using MP2[26] and coupled cluster single and double excitation (CCSD) theories[27] using 6-31++g(d, p) basis sets of the atoms. The geometry of the dimers was fully optimized, and the minimum energy structures in the respective cases were confirmed through frequency calculations. Similar calculations were carried out on the monomers of formic acid (*cis*- and *trans*-conformers) and formamide. The results were used to compute the binding energies (ΔE^{B}), enthalpy (ΔH^{B}_{298}), and Gibbs free energy (ΔG^{B}_{298}) of binding (at 298 K) of the respective dimers with counterpoise (CP) and zero-point energy (ZPE) corrections. The calculations of thermodynamic properties have been carried out by applying the ideal gas, rigid rotator, and harmonic oscillator approximations.[28]

The computed vibrational frequencies of the dimers (as well as monomers) and their binding energies (ΔE^{B}, ΔH^{B}_{298}, ΔG^{B}_{298}) are explicitly corrected at the MP2/6-31++g(d, p) level for the effect of anharmonicity using Barone's formalism.[29,30] The corrections of the respective parameters at the CCSD level were carried of using the anharmonicity constants (x_{ij}) and ZPE corrections (for the anharmonic effect) obtained through MP2/6-31++g(d, p) calculations. In the case of several formamide dimers (characterized by all real fundamentals within harmonic approximations), the computed anharmonicity-corrected frequencies generated imaginary values for a few low-frequency modes at the MP2/6-31++g(d, p) level. In such cases the anharmonicity corrections were computed using the anharmonicity constants (x_{ij}) and ZPE corrections from the density functional theory (DFT).[31] The standard B3LYP[32−34] functional was used, and the needed anharmonicity parameters were generated after full geometry optimizations of the respective dimers (using 6-31++g(d, p) basis sets). Thus these approximated results should be considered for the comparison purposes only as they have incurred error for the anharmonicity corrected terms, but it would be found that these approximations still keep the computed values within reasonable accuracy with respect to the available experiment.

The computed energy values were further refined using single point energy calculations on the optimized structures at the MP2 and CCSD levels using aug-cc-pvtz basis set of atoms. The respective ΔH^{B}_{298} and ΔG^{B}_{298} values were approximated from the computed values at the MP2/6-31++g(d, p) and CCSD/6-31++g(d, p) levels using the following relation 1.

$$\Delta X^{B}_{298} = \Delta X^{B}_{298}(\text{6-31++g(d, p)}) + [\Delta E^{B}(\text{aug - cc - pvtz}) - \Delta E^{B}(\text{6-31++g(d, p)})], \quad (X = H, G) \tag{1}$$

The second term in eq 1 accounts for the higher electron-correlation effect on the energy values (due to the use of aug-cc-pvtz basis sets in the present calculations). The computed

thermodynamic parameters viz. ΔE^{B}, ΔH^{B}_{298}, and ΔG^{B}_{298} in eq 1 contain only the harmonic ZPE, and they were further improved using the anharmonicity-corrected ZPEs[29,30] from the 6-31++g(d, p) basis set computations. The results have been compared against the fully optimized data of the lowest energy formic acid and formamide dimers using aug-cc-pvtz basis set computations, and such approximations were found to be quite satisfactory (see section III A). A single-point coupled cluster calculations with triple excitations (CCSD(T))[35] were carried out on the CCSD-optimized dimer geometries to improve accuracy of the computed binding energies using similar strategy of eq 1. The reliability of the computed energies was further gauged against the results from G4MP2,[36] G2MP2,[37] and CBS-QB3[38] techniques.

All the computations were carried out using Gaussian 09 code,[39] and graphics presented in the manuscript were obtained through Gauss View 5 software.[40]

III. RESULTS

a. Structural and Vibrational (High Frequency Modes) Characteristics of Formic Acid Dimers. The optimized structures (at the CCSD level) of formic acid dimers are shown in Figure 1. Dimers formed through six *trans*−*trans* (TT-1 to TT-6) and five *trans*−*cis* (TC-1 to TC-5) combinations of monomers are presented. These structures have previously been computed at the MP2 level.[12,15,16] In the present manuscript the interest is on the effect of anharmonicity on the binding energies and vibrational frequencies of these dimers. The geometries of the dimers at the MP2 and CCSD levels are compared (in terms of hydrogen bonding distances) in Table 1s of the Supporting Information. All the structures in Figure 1 are arranged according to their relative energies with respect to the most abundant TT-1 (for *trans*−*trans*) and TC-1 (for *trans*−*cis*) dimers (Table 1).

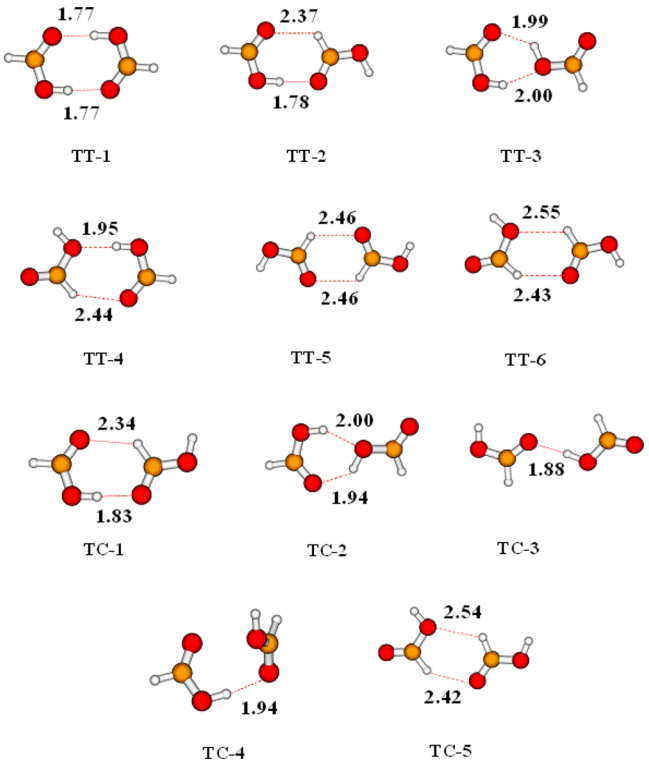

Figure 1. Optimized structures of formic acid dimers (at the CCSD level) with the computed hydrogen-bond distances (Å). These dimers are formed through *trans*−*trans* (TT-1 to TT-6) and *trans*−*cis* (TC-1 to TC-5) combinations of the monomers. The structures are similar at the MP2 level, and the corresponding hydrogen-bond distances are available in Table 1s of the Supporting Information.

Table 1. Relative Energies (ΔE) and Anharmonicity-Corrected Binding (ΔE^{B}) Energies (Including Enthalpy (ΔH^{B}_{298}) and Gibbs Free Energies (ΔG^{B}_{298}) of Binding) of the Various Isomers of Formic Acid Dimer (All in kcal/mol)[a,b]

dimers	calculation level	ΔE	ΔE^{B}	ΔH^{B}_{298}	ΔG^{B}_{298}
TT-1	MP2	0.00	−13.35	−13.49	−2.34
			(−13.39)[c]	(−13.71)	(−2.67)
(C_{2h})	CCSD	0.00	−12.45	−12.59	−1.44
			(−12.22)[c,d]		
	CCSD(T)	0.00	−13.23	–	–
TT-2	MP2	6.48	−7.21	−7.59	1.92
(C_s)	CCSD	5.79	−7.34	−7.37	2.62
	CCSD(T)	6.10	−7.82	–	–
TT-3	MP2	8.60	−5.80	−5.67	3.26
(C_1)	CCSD	8.61	−4.81	−4.84	5.07
	CCSD(T)	8.59	−5.62	–	–
TT-4	MP2	9.96	−4.70	−5.01	4.20
(C_1)	CCSD	9.20	−4.51	−4.21	4.28
	CCSD(T)	9.60	−4.92	–	–
TT-5	MP2	12.08	−3.19	−2.68	4.81
(C_{2h})	CCSD	11.00	−3.32	−2.74	4.81
	CCSD(T)	11.58	−3.52	–	–
TT-6	MP2	13.06	−2.42	−2.45	5.16
(C_s)	CCSD	12.09	−2.36	−1.78	5.17
	CCSD(T)	12.66	−2.66	–	–
TC-1	MP2	9.80	−4.23	−4.13	5.45
(C_s)	CCSD	9.19	−3.92	−3.98	5.67
	CCSD(T)	9.49	−4.41	–	–
TC-2	MP2	10.61	−3.52	−3.12	6.06
(C_1)	CCSD	10.13	−3.08	−3.33	5.69
	CCSD(T)	10.36	−3.66	–	–
TC-3	MP2	12.37	−2.03	−1.57	4.93
(C_1)	CCSD	11.72	−1.78	−1.31	5.55
	CCSD(T)	12.03	−2.25	–	–
TC-4	MP2	12.68	−2.00	−1.98	7.13
(C_1)	CCSD	11.90	−1.82	−1.81	7.23
	CCSD(T)	12.44	−2.09	–	–
TC-5	MP2	17.09	1.68	2.31	9.26
(C_s)	CCSD	16.13	1.72	2.35	9.35
	CCSD(T)	16.66	1.43	–	–

[a]All the binding energies (ΔE^{B}, ΔH^{B}_{298}, and ΔG^{B}_{298}) are after counterpoise corrections and inclusion of zero-point energies. [b]The strategy for the computation of anharmonicity corrected energies at the CCSD and CCSD(T) levels is discussed in the text. [c]Results from fully optimized geometry using aug-cc-pvtz basis sets. Anharmonicity corrections are taken from 6-31++g(d, p) results. [d]Computed using zero-point energy corrections from the MP2/aug-cc-pvtz results.

Most of these dimers are planar with only one notable exception (TC-4). This dimer was predicted to be planar in previous caculations.[15] Our present computations (both MP2 and CCSD) show that TC-4 generates imaginary frequency if planarity is imposed. The computed vibrational frequencies of this non-planar dimer also reproduce the experimental data quite satisfactorily (Table 2). Moreover, the dimers TT-4, TT-5, and TC-2 also show slight deviation from planarity in their fully optimized structures (both at the MP2 and CCSD levels).

Table 2. Calculated Vibrational Frequencies (cm^{-1}) of Different Formic Acid Dimers at the MP2 and CCSD Level of Theories (Using 6-31++g(d, p) Basis Sets)[a]

formic acid dimers	theory level and Expt. data	frequencies			
		ν(OH)	ν(C=O)	CO−COH def.	τ(COH)
TT-1	MP2	3119	1746	1361, 1226, 1108	929
	CCSD	3264	1785	1426, 1231, 1105	914
	Expt.	3072	1728	1224, 1225	939
TT-2	MP2	3584, 3288	1752, 1722	1338, 1247, 1178, 1131	849, 671
	CCSD	3584, 3226	1805, 1766	1378, 1275, 1214, 1166	906, 694
	Expt.	3540, 3184	1748	1180, 1131	868, 658
TT-3	MP2	3494, 3398	1769, 1743	1252, 1157, 1105	786, 696
	CCSD	3508, 3416	1780, 1750	1282, 1167, 1088	800, 625
	Expt.	3423	1771, 1734	1159, 1110	–
TT-4	MP2	3590, 3454	1770, 1752	1322, 1190, 1157	752, 530
	CCSD	3634, 3534	1818, 1797	1343, 1129, 1086	799, 635
	Expt.	3544, 3387	1774, 1750	1154, 1074	–
TT-5	MP2	3590	1757	1230, 1114	650
	CCSD	3632	1801	1255, 1121	639
	Expt.	–	1756	1092	642
TT-6	MP2	3590, 3588	1762, 1755	1285, 1109, 1088	637, 634
	CCSD	3632, 3630	1811, 1799	1310, 1130, 1110	626, 623
	Expt.	3537	1765	1115	661, 667
TC-1	MP2	3652, 3257	1767, 1734	1251, 1184, 1140	858, 540
	CCSD	3687, 3257	1813, 1775	1276, 1196, 1152	843, 525
	Expt.	3604, 3115	1767	1259, 1186, 1143	875, 550
TC-2	MP2	3447, 3393	1795, 1738	1334, 1235, 1159, 1095	767, 672
	CCSD	3529, 3489	1849, 1780	1354, 1256, 1173, 1113	747, 653
	Expt.	3411	1793	1241, 1155	–
TC-3	MP2	3586, 3469	1793, 1748	1308, 1243, 1135, 1131	710, 664
	CCSD	3826, 3514	1844, 1788	1331, 1265, 1148, 1148	689, 654
	Expt.	3363	1787	1338, 1151	–
TC-4	MP2	3653, 3414	1792, 1749	1245, 1159, 1124	759, 484
	CCSD	3687, 3614	1834, 1788	1272, 1172, 1138	731, 472
	Expt.	3406	1797, 1726	1254, 1158	–
TC-5	MP2	3654, 3586	1791, 1762	1233, 1103, 1083	638, 506
	CCSD	3687, 3629	1841, 1811	1260, 1118, 1105	627, 490
	Expt.	3603	1807	1268, 1119, 1060	686, 534

[a]The anharmonicity correction at the CCSD level is discussed in the text. The reported values are after anharmonicity corrections. The available experimental (Expt.) (see footnote *b*) values are also included in the table for comparison. [b]References 15 and 16.

The computed ΔE^B values of formic acid dimers at the MP2, CCSD, and CCSD(T) levels are presented in Table 1. They are computed by considering the dimers to be formed from the lowest energy *trans*-conformer of the formic acid. Thus in the cases of *trans*−*trans* dimers, the ΔE^Bs are an approximate measure of the respective hydrogen bond energies. In the case of *trans*−*cis* dimers, these ΔE^B values should be added with the energy difference between the *trans*- and *cis*-conformers of formic acid (isomerization energy; Table 2s, Supporting Information) to compute their approximate hydrogen bond energies. Only the anharmonicity-corrected ΔE^Bs are presented, as in most of the cases the maximum increase of binding energies due to the anharmonicity effect is ∼0.12 kcal/mol. The computed values are also similar at the different level of theories, although these energies are slightly underestimated at the CCSD level. These are rectified at the CCSD(T) level, and the binding energies are similar to those at the MP2 level. In view of the previously computed interaction energies,[15,16] these binding energies are quite consistent. Table 1 also contains ΔH^B_{298} and ΔG^B_{298} of formic acid dimers using CP and ZPE corrections (with respect to their formation from the *trans*-conformer of formic acid) at the MP2 and CCSD levels. The computed ΔH^B_{298} values are similar to those of ΔE^Bs, as the thermal corrections in such cases are small. The entropic contribution to $T\Delta S$ (T: temperature (298 K here); S: entropy) is quite high in such dimer formations, and this unfavorable term causes only the most abundant (TT-1) dimer to be stable at room temperature (negative ΔG^B_{298} after anharmonicity correction). All the other dimers are unstable at this temperature according to the computed ΔG^B_{298} values. This observation is supported by the fact that the less abundant dimers of formic acid are obtained either at very low temperature (below 25 K; *trans*−*trans* dimers) or through vibrational excitations (*trans*−*cis* dimers). Similar ΔG^B_{298}-based observations were also made previously by Aquino and co-workers[41] for several weakly hydrogen bonded systems.

The computed high-frequency modes of formic acid dimers are presented in Table 2 at the MP2 and CCSD levels of theory. The frequencies are presented with anharmonicity corrections. The anharmonic vibrations are obtained directly at the MP2 level from the optimized anharmonicity corrected geometries using Barone's technique.[29,30] The vibrations at the CCSD level are corrected for anharmonicity using the following relation 2

$$\nu_{anh}^{CCSD} = \nu_{h}^{CCSD} - [\nu_{h}^{MP2} - \nu_{anh}^{MP2}] \quad (2)$$

where ν_{anh} and ν_h are the anharmonic and harmonic vibrations for a particular mode at the CCSD/MP2 level. These approximate results are less accurate than those at the MP2 level, but they are still comparable with experiment (Table 2).

The dimerization of formic acid influences the vibrational frequencies of the monomer subunits. These are either red- or blue-shifted. The anharmonicity corrected vibrational modes (comparable modes with respect to the dimers) of *cis*- and *trans*-formic acid are presented in Table 2s along with the

dx.doi.org/10.1021/ct300889b | J. Chem. Theory Comput. 2013, 9, 1016−1026

available experimental data, and it can be easily seen that the ν(OH), ν(CO), CO−COH def. (deformation), and τ(COH) modes are either red- or blue-shifted. These features have been discussed in earlier papers,[15,16] and predictions have been made that the strongest redshift of ν(OH) (∼−463 cm^{-1}) could be related to the formation of the most stable (TT-1) dimer. In the present case, the respective anharmonicity-corrected vibrational modes present similar features. The advantage of such computed values is that they are more accurate than harmonic frequencies (when compared with experiments) and thus such comparisons are more realistic.

b. Structural and Vibrational (High Frequency Modes) Characteristics of Formamide Dimers. Formamide does not possess the rotamerism property of formic acid. This limits the formation of probable dimers to five (Figure 2). Two of them (FMAD-A and FMAD-C) have been characterized through infrared spectra, and the presence of FMAD-B has been predicted.[19] The rest of them are predicted from theoretical calculations only. We have optimized all five dimers at the MP2 and CCSD levels (Figure 2). The hydrogen-bonding distances for the CCSD/6-31++g(d, p) computations are presented in the figure, while the hydrogen bonding distances for MP2-optimized geometries are shown in Table 1s. These hydrogen bonds are formed through NH···O, NH···N, or CH···O interactions. Obviously the CH···O interactions are the weakest. This is reflected in the computed binding energies of the dimers. The relative energy (ΔE) and the anharmonicity-corrected binding energies (ΔE^{B}, ΔH^{B}_{298}, and ΔG^{B}_{298}) are presented in Table 3. FMAD-A is the most abundant and strongly bound among these dimers.

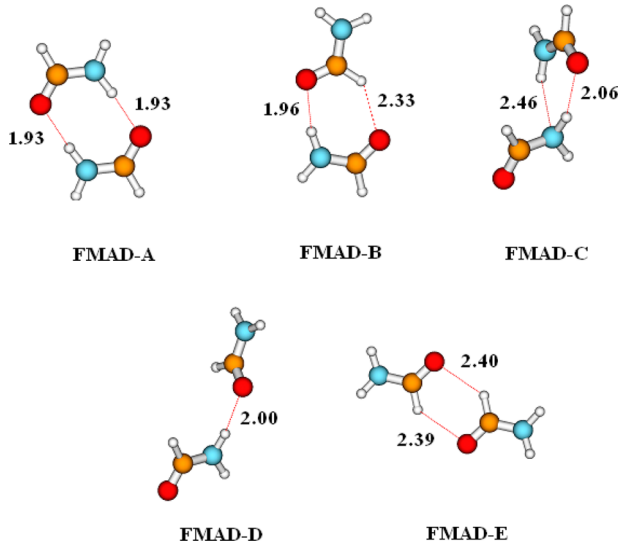

Figure 2. Optimized structures of formamide dimers (at the CCSD level) with the computed hydrogen-bond distances (Å). These dimers are formed through different orientations of the monomers (FMAD-A to FMAD-E). The structures are similar at the MP2/DFT-B3LYP level of computations and the corresponding hydrogen-bond distances are available in Table 1s of the Supporting Information.

The anharmonicity corrections for the binding energy calculations were employed through DFT/B3LYP calculations (except FMAD-C) as the MP2 calculations with anharmonicity effect generated a few imaginary frequencies (discussed in Section II). The geometry of the respective dimers was fully optimized at the DFT/B3LYP/6-31++g(d, p) level to compute

Table 3. Relative Energies (ΔE) and Anharmonicity-Corrected Binding (ΔE^{B}) Energies (Including Enthalpy (ΔH^{B}_{298}) and Gibbs Free Energies (ΔG^{B}_{298}) of Binding) (All in kcal/mol) of the Various Isomers of Formamide Dimer (FMAD)[a,b]

dimers	calculation level	ΔE	ΔE^{B}	ΔH^{B}_{298}	ΔG^{B}_{298}
FMAD-A	MP2	0.00	−12.86	−12.52	−4.69
			(−11.79)[c]	(−12.42)	(−0.96)
(C_{2h})	CCSD	0.00	−12.12	−11.73	−3.12
			(−12.12)[c,d]		
	CCSD(T)	0.00	−12.92	–	–
FMAD-B	MP2	4.88	−8.45	−7.98	0.82
(C_1)	CCSD	4.42	−8.12	−7.64	1.20
	CCSD(T)	4.70	−8.66	–	–
FMAD-C	MP2	7.04	−6.30	−6.00	2.76
(C_1)	CCSD	6.71	−5.82	−3.74	2.91
	CCSD(T)	6.98	−6.36	–	–
FMAD-D	MP2	7.95	−5.91	−5.23	1.42
(C_1)	CCSD	7.91	−5.15	−4.43	2.06
	CCSD(T)	8.47	−5.43	–	–
FMAD-E	MP2	9.70	−4.26	−2.06	2.92
(C_{2h})	CCSD	8.87	−4.29	−3.58	1.65
	CCSD(T)	9.44	−4.57	–	–

[a]All the binding energies (ΔE^{B}, ΔH^{B}_{298}, and ΔG^{B}_{298}) are after counterpoise corrections and inclusion of zero-point energies. [b]The strategy for the computation of anharmonicity corrected energies (using corrections through DFT/B3LYP technique) are discussed in the text. [c]Results from fully optimized geometry using aug-cc-pvtz basis sets. Anharmonicity corrections are taken from 6-31++g(d, p) results. [d]Computed using zero-point energy corrections from the MP2/aug-cc-pvtz results.

anharmonicity effect, and the corrections for binding energies (ZPE) were directly included to the MP2 and CCSD results. The hydrogen-bonding distances of these optimized structures are available in Table 1s, and they are not different from MP2 and CCSD results. The anharmonicity effect increases the ΔE^{B} values by ∼0.2 kcal/mol in most of the cases, and the ΔE^{B} of the most stable FMAD-A is similar to the TT-1 dimer of formic acid (difference is ∼0.5 kcal/mol). Like formic acid dimers, the ΔH^{B}_{298} of FMADs are similar to their ΔE^{B} values, while the entropic effects are quite substantial to make ΔG^{B}_{298} small for these dimers. In fact from ΔG^{B}_{298} consideration, FMAD-A is relatively the most stable dimer (negative ΔG^{B}_{298} value) at room temperature (298 K). This is supported by the fact that the other two dimers, which are assigned experimentally, were detected at very low temperature (∼10 K) in argon or xenon matrices. Table 3 also contains the binding energies for the fully optimized FMAD-A geometry using aug-cc-pvtz basis sets. The results show that the ΔE^{B}, using approximations through eq 1, is overestimated by ∼1 kcal/mol. This is also evident from the comparison with G4MP2, G2MP2, and CBS-QB3 results (discussed later in Table 7s; Supporting Information).[42] The ΔG^{B}_{298} is also overestimated. The error in this case is occurring due to the use of eq 1 for such calculations through the use of already overestimated 6-31++g(d, p) results.

The dimerization of formamide, like formic acid, influences the vibrational frequencies of the monomer subunits. The computed anharmonicity-corrected frequencies as presented in Table 4 show that they are either red- or blue-shifted with respect to those of monomer frequencies (Table 2s). The anharmonic corrections on the MP2 and CCSD results (Table 4) were included through

Table 4. Calculated Vibrational Frequencies (cm^{-1}) of Different Formamide Dimers (FMAD) at the DFT/B3LYP, MP2,[a,b] and CCSD Level[c] of Theories

		frequencies					
FMAD	theory level and Expt. data	$\nu_{as}(NH_2)$[d]	$\nu_s(NH_2)$[d]	ν(C−H)	ν(C═O)	ν(C−N)	$\tau(NH_2)$
FMAD-A	DFT	3498	3140	2858	1742	1299	811
	MP2	3515	3276	2931	1758	1353	938
	CCSD	3523	3334	2924	1778	1321	927
	Expt.	3515	3131 (3216)	2864	1728	1313	818
FMAD-B	DFT	3538, 3510	3418	2934	1747	1290	763, 593
	MP2	3636, 3596	3496, 3290	3038, 2867	1756, 1727	1311, 1266	736, 585
	CCSD	3625, 3603	3505, 3344	3040, 2863	1779, 1747	1315, 1269	727, 578
FMAD-C	MP2	3616, 3565	3471, 3431	2952, 2954	1753, 1745	1280, 1266	710, 640
	CCSD	3622, 3572	3492, 3470	2945, 2951	1787, 1769	1284, 1272	689, 630
	Expt.	3522	3353, 3219	–	1731, 1721	1296	835, 769
		–	(3369, 3355)	–	–	–	769
FMAD-D	DFT	3543, 3501	3424, 3389	2891, 2750	1751, 1742	1209, 1256	692, 561
	MP2	3632, 3584	3502, 3464	2990, 2856	1754, 1751	1236, 1278	701, 556
	CCSD	3632, 3595	3512, 3507	2984, 2854	1782, 1777	1239, 1283	679, 548
FMAD-E	DFT	3535, 3535	3416, 3416	3030, 3025	1747, 1723	1277, 1262	583, 581
	MP2	3619, 3619	3491, 3490	3003, 3000	1752, 1732	1243, 1268	573, 572
	CCSD	3616, 3616	3499, 3458	3005, 3003	1780, 1758	1247, 1272	565, 564

[a]The reported values are after anharmonicity corrections. The available experimental (Expt.) (ref 19) values are also included in the table for comparison. [b]The MP2 results with anharmonicity effect (except FMAD-C) generated imaginary frequencies for a few low frequency modes (although harmonic values are all real). Thus DFT/B3LYP data have been included for comparison. The results for these high-frequency modes are similar although DFT/B3LYP data are slightly better. [c]The anharmonicity corrections for the CCSD data have been carried out using eq 1. [d]ν_{as} and ν_s respectively represent the asymmetric and symmetric stretching modes.

DFT/B3LYP results using the relation similar to eq 1. The strongest red-shift of $\nu_s(NH_2)$ (∼−387 cm^{-1}) and $\nu_{as}(NH_2)$ (−171 cm^{-1}) could be related to the formation of the most stable (FMAD-A) dimer. There are several other features of the vibrational frequencies, which are responsible for the stiffness of such bonds. These are related to the low-frequency modes of these dimers.

c. Low-Frequency Modes of Formic Acid and Formamide Dimers. The low-frequency modes of the most stable formic acid dimer (TT-1) was investigated in detail (100−750 cm^{-1}) under jet-cooled, vacuum-isolated conditions by Xue et al.[25] They have assigned the Raman-active fundamentals, overtones, and combination bands involving the in-plane and out-of-plane bending and stretching vibrations of the hydrogen bonds. Table 5 contains the computed first six fundamentals, their overtones, and several of their combination bands. The first six fundamentals are presented in Figure 3 (computed at the MP2 level). The modes involving *u*-symmetry (two A_u and one B_u) are IR-active, while the modes involving *g*-symmetry (two A_g, and one B_g) are Raman-active (because of C_{2h} symmetry of TT-1). The lowest fundamental (ν_1, A_u) was assigned from the detection of the overtone ($[2\nu_1]$, A_g) band in the experiment and is properly reproduced in our theoretical approaches (Table 5). All the anharmonicity corrected low-frequency fundamentals (ν_i), their overtones ($[2\nu_i]$), and the mixed modes ($[\nu_i\nu_j]$) are dependent on the harmonic frequencies (ω_i) and anharmonicity constants (x_{ij}) through the following relations[30]

$$\nu_i = \omega_i + 2x_{ii} + \frac{1}{2}\sum_{j\neq i} x_{ij} \tag{3}$$

$$[2\nu_i] = 2\omega_i + 6x_{ii} + \sum_{j\neq i} x_{ij} = 2\nu_i + 2x_{ii} \tag{4}$$

$$[\nu_i\nu_j] = \nu_i + \nu_j + x_{ij} \tag{5}$$

These anharmonicity corrected frequencies are directly computed at the MP2 level, and the extracted x_{ij} values at this level are used to compute the corresponding frequencies at the CCSD levels. The fundamentals presented in Table 5 at the CCSD level are computed using eq 2, while eqs 4 and 5 are used to compute the overtone and mixed frequencies. The computed results at both MP2 and CCSD levels are in good agreement with the experimental results. It is to be noted that the experimental low-frequency modes were assigned according to the Herzberg notation.[25,43] In the present manuscript we have assigned them starting from the lowest fundamentals (as ν_1, ν_2,...). In this way it is easier to compare these modes with other dimers (especially those isomers having C_1 symmetry).

The lowest energy formamide dimer (FMAD-A) is very similar to TT-1 structurally. Both of them are in C_{2h} symmetry, and the binding energies are also comparable. Thus we have compared the low-frequency vibrations of FMAD-A with those of TT-1 (Table 5) in order to address the origin of such similarities. Because of the problem of computing the anharmonicity corrected modes at the MP2 level (as discussed earlier), we have computed the frequencies at the DFT/B3LYP level and used equations similar to (2), (4), and (5) to compute ν_i, $[2\nu_i]$, and $[\nu_i\nu_j]$ frequencies at the CCSD level. The results at the MP2 level are similar to those of the CCSD, and they are not discussed here. The first six low-frequency fundamentals (at the DFT/B3LYP level) are presented in Figure 4. As in the case of TT-1, three of the modes (two A_u, and one B_u) are IR-active, while the other three modes of *g*-symmetry (two A_g, and one B_g) are Raman-active. The displacement vectors of these fundamentals (Figure 4) are similar to those of TT-1 (Figure 3), although the magnitudes of these frequencies are lower due to the difference of the nature of the atoms involved

Table 5. Comparison of the Low Frequency Fundamentals (cm^{-1}), Their Overtones (cm^{-1}), and Anharmonicity Constants (x_{ij}, cm^{-1}) of the Lowest Energy Dimers of Formic Acid (TT-1) and Formamide (FMAD-A) Computed at the MP2/DFT[a] and CCSD Level of Theories Experimental Data[b] in the Case of TT-1 Are Included in Table for Comparison

	mode[c]		fundamental			mode		overtone			x_{ij}	
dimer	calc.	Expt.[d]	MP2/DFT	CCSD[e]	Expt,	calc.	Expt.[d]	MP2/DFT	CCSD[e]	Expt.	calc.	Expt
TT-1	ν_1 (A_u)	ν_{16} (A_u)	65.4	67.0	69.2	$2\nu_1$ (A_g)	$2\nu_{16}$ (A_g)	132.0	134.7	139	0.36	0
(C_{2h})	ν_2 (A_u)	ν_{15} (A_u)	162.0	156.0	168.5	$2\nu_2$ (A_g)	$2\nu_{15}$ (A_g)	323.0	313.4	336	0.71	−1
	ν_3 (B_u)	ν_{24} (B_u)	237.0	225.0	248.0		n.o					
	ν_4 (A_g)	ν_8 (A_g)	182.0	177.0	194.0	$2\nu_4$ (A_g)	$2\nu_8$ (A_g)	362.0	352.2	386	−0.9	−1
	ν_5 (A_g)	ν_9 (A_g)	150.0	156.0	161.0	$2\nu_5$ (A_g)	$2\nu_9$ (A_g)	299.0	311.0	319	−0.49	−2
	ν_6 (B_g)	ν_{12} (B_g)	234.0	233.0	242.0	$2\nu_3$ (B_g)	$2\nu_{12}$ (B_g)	466.0	464.5	482	−0.73	−1
						$\nu_5 + \nu_3$ (B_u)	$\nu_9 + \nu_{24}$ (B_u)	384.8	378.8	395	−2.17	−20[h]
						$\nu_6 + \nu_5$ (B_g)	$\nu_{12} + \nu_9$ (B_g)	382.3	386.9	400	−2.02	−3
						$\nu_6 + \nu_4$ (B_g)	$\nu_{12} + \nu_8$ (B_g)	414.1	408.1	435	−1.92	−1
						$\nu_6 + \nu_1$ (B_u)	$\nu_{12} + \nu_{16}$ (B_u)	300.3	300.9	311	0.92	0
FMAD-A[f]	ν_1 (A_u)	–	64	54	–	$2\nu_1$ (A_g)	–	128.0	108.3	–	0.16	–
(C_{2h})	ν_2 (A_u)	–	144	34?[g]	–	$2\nu_2$ (A_g)	–	288.1	–	–	0.39	–
	ν_3 (B_u)	–	195	185	–	$2\nu_3$ (A_g)	–	384.4	363.4	–	−3.29	–
	ν_4 (A_g)	–	134	120	–	$2\nu_4$ (A_g)	–	260.3	238.9	–	−0.56	–
	ν_5 (A_g)	–	154	149	–	$2\nu_5$ (A_g)	–	304.0	294.1	–	−1.95	–
	ν_6 (B_g)	–	194	40?[g]	–	$2\nu_3$ (B_g)	–	392.3	–	–	2.4	–
						$\nu_3 + \nu_4$ (B_u)		326.4	302.2	–	−2.77	–
						$\nu_6 + \nu_5$ (B_g)		346.9		–	−0.83	–
						$\nu_6 + \nu_1$ (B_u)		259.7		–	2.12	–

[a]The results of FMAD-A are presented at the DFT/B3LYP and CCSD levels. See the texts for the details. [b]Reference 25. [c]All of the low-frequency fundamentals are presented in Figure 3 (TT-1) and Figure 4 (FMAD-A) respectively. [d]The assignments of the experimental data[25] are according to Herzberg's notation. The computed values are assigned from the lowest to the higher frequencies. [e]CCSD data are presented using the correction factors and x_{ij} values from the MP2/DFT computations. Thus these results carry higher error bars. See the text for the details. [f]The FMAD-A data are presented using DFT/B3LYP and CCSD level of theories. The anharmonicity corrections for the CCSD data are using x_{ij} values from the DFT/B3LYP computations. [g]These computed parameters are not very reliable. [h]The experimental data are from unresolved gas-phase band and considered as approximate.

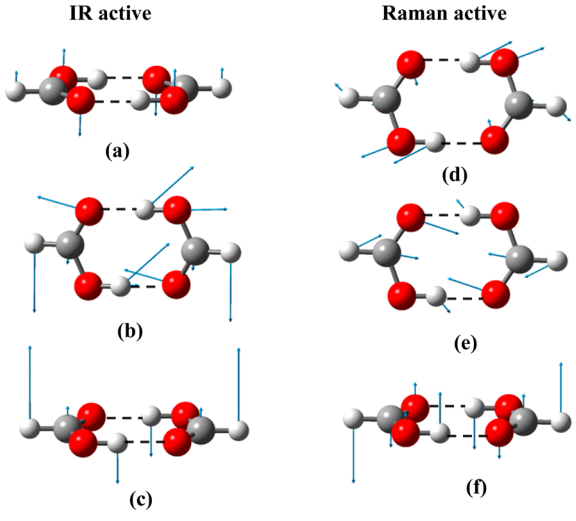

Figure 3. First six low-frequency IR and Raman-active fundamentals of TT-1 dimer computed at the MP2 level. The nuclear displacements of these modes are shown for comparison with the lowest energy formamide (FMAD-A) dimer. The IR-active modes are (a) twisting (A_u, 65.4 cm^{-1}), (b) in-plane-bending (B_u, 162 cm^{-1}), and (c) out-of-plane bending (A_u, 237 cm^{-1}). The Raman-active modes include (d) stretching (A_g, 182 cm^{-1}), (e) in-plane-bending (A_g, 150 cm^{-1}), and (f) out-of-plane bending (B_g, 237 cm^{-1}).

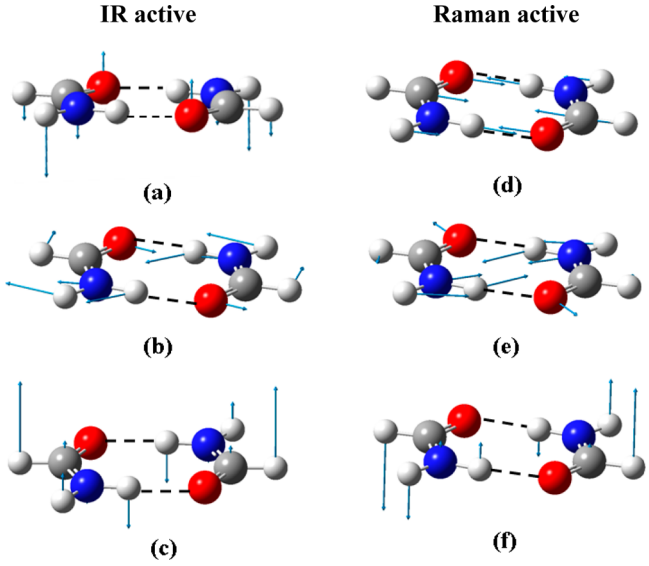

Figure 4. First six low-frequency IR and Raman-active fundamentals of FMAD-A dimer computed at the DFT/B3LYP level together with the corresponding nuclear displacements. The IR-active modes are (a) twisting (A_u, 64 cm^{-1}), (b) in-plane-bending (B_u, 144 cm^{-1}), and (c) out-of-plane bending (A_u, 195 cm^{-1}). The Raman-active modes include (d) stretching (A_g, 134 cm^{-1}), (e) in-plane-bending (A_g, 154 cm^{-1}), and (f) out-of-plane bending (B_g, 194 cm^{-1}).

in hydrogen-bonding interactions. We have further computed the various low-frequency modes of other formic acid (TT2 to TC5, Figure 1) and formamide (FMAD-B to FMAD-E, Figure 2) to understand their roles to control the strength of the hydrogen-bonds in the respective dimers, and they are available in the Supporting Information (Tables 4s and 5s). Except TT-2, there are no experimental data on the low-frequency modes of

dx.doi.org/10.1021/ct300889b | J. Chem. Theory Comput. 2013, 9, 1016−1026

these isomers. The out-of-plane bending mode (o.p.bend, ν_6, Table 4s) of this dimer (TT-2) was assigned to be 213 cm^{-1},[14] and it matches with our computed result (206 cm^{-1}) quite well.

IV. DISCUSSIONS

a. Correlation of Binding Energies with the Contributing High- and Low-Frequency Modes. Vibrational spectra of dimeric hydrogen-bonded systems provide information on the local properties of the hydrogen-bonded groups. The stretching bands of the -OH or -NH_2 groups show substantial red-shift with respect to the corresponding monomer frequencies, and the intensity (I, km/mole)) of such modes are also highly enhanced. For example the computed intensities of ν(OH) (ν = 3119 cm^{-1}, I = 1998) and ν(CO) (ν = 1746 cm^{-1}, I = 787) of the TT-1 isomer show a huge enhancement with respect to the corresponding frequencies of *trans*-formic acid (ν(OH) = 3592 cm^{-1} (I = 75); ν(CO) = 1766 cm^{-1} (I = 348)). The case is similar for the formamide dimer (FMAD-A) also ($\nu_s(NH_2)$ = 3276 cm^{-1} (I = 1078), and ΔI = 1019). The experimental values in such cases are also comparable.[15,19] These properties enable such modes to be considered as marker bands (fingerprint) for such dimers.[13] It has also been demonstrated experimentally that the anharmonic coupling of the high-frequency stretching modes of such groups to the low-frequency interdimer stretch and twist modes directly modulates the hydrogen bonding strength of the high-frequency modes.[44,45] The experiment on the low-frequency mode analysis of the most stable formic acid dimer (TT-1)[25] actually substantiated such a view.

Analysis of the computed vibrational characteristics of various formic acid and formamide dimers reveals several interesting features. The intensities of the ν(OH) and $\nu_s(NH_2)$ modes of formic acid and formamide dimers regularly decrease with respect to their binding characteristics (Table 3s, Supporting Information). Figures 5A and 5B show that such intensities are linearly correlated with the respective hydrogen bond energies (ΔE^{HB}) of such dimers, as the modes involved [ν(OH) and $\nu_s(NH_2)$] are known to be responsible for hydrogen-bond formation in the respective cases and the corresponding intensities are approximately proportional to the force involved in such bond formation. The dimer TC-5 was not considered in Figure 5A because of its repulsive (positive) hydrogen-bond energy. The -NH_2 group is not involved in hydrogen-bonding in the least stable formamide dimer FMAD-E (Figure 2; Table 3), but the linear correlation of the intensity of this mode with the rest of the formamide dimers (Figure 5B) is not accidental, as the ΔE^{HB} also represents ΔE^{B} of such dimers.

In the case of low-frequency mode analysis, there are six fundamentals (Tables 5, 4s, and 5s), which could be considered for similar correlation. Of these, only the intensities of the in-plane-bending or stretch−bend (in-plane) modes of the isomers of formic acid and formamide dimers show a regular change with respect to their binding strengths. These modes are shown in Figures 1s and 2s of the Supporting Information along with their respective frequencies and intensities. These modes are all IR-active and represent the specific hydrogen-bonding dissociation features of such dimers. Figures 5C and 5D show that in the case of formic acid and formamide dimers the intensity of such modes correlates linearly with the respective ΔE^{B} values. Only the corresponding intensity of TC-5 (Figure 5C) does not fall into such linear correlation as its binding energy is positive.

The ΔE^{B} of the *trans*−*trans* formic acid (TT-1 to TT-6) and formamide (FMAD-A to FMAD-E) dimers are same as their ΔE^{HB} values. It has been found further that the ΔE^{B}s of the *trans*−*trans* and *trans*−*cis* (TC-1 to TC-5) dimers of formic acid show two separate linear correlations with respect to the intensities of their respective ν(OH) frequencies (not shown in the manuscript) as $\Delta E^{B} \neq \Delta E^{HB}$ for the *trans*−*cis* dimers. Thus the correlations in Figure 5 clearly show how the specific low-frequency modes are involved (together with the high frequency ν(OH)/$\nu_s(NH_2)$ modes) to modulate the binding strengths of such dimers. It further shows that the low-frequency modes involved in correlation of the lowest energy dimers of both formic and formamide are similar, and such modes are responsible for the similar relative stabilities of these two dimers.

b. The Empirical Additive Relation of Binding Energies Involving Formic Acid and Formamide Dimers. The linear dependence of the intensities of both high- and low-frequency modes of formic acid and formamide dimers with their binding energies indicates that an additivity relation of binding energies (as well as the corresponding intensities) might exist among the dimers due to transferable local character of the individual hydrogen-bonding fragments. In the case of binding energies, these additivity relations could be sought through analysis of the local hydrogen-bonding/binding energies of the fragments involved. Let us first consider the case of formic acid dimers and designate the binding energies of the fragments involved in local hydrogen-bonding as $E_{X\cdots Y}$ (where X and Y are the atoms or the groups involved in hydrogen-bonding). In the case of formic acid dimers (Figure 1) these fragments are OH···O, CH···O, OH···O(H), and CH···O(H) (the hydrogen within parentheses belongs to the OH group not involved in hydrogen-bonding), and the local binding energies could be obtained from the individual binding energies of the dimers from Table 1. The binding energies at the MP2 level are only being considered in the present context. The dimers TT-1 and TT-5 have double hydrogen-bonds formed through OH···O and CH···O fragments respectively, and thus from their respective ΔE^{B} (Table 1) the $E_{OH\cdots O}$ and $E_{CH\cdots O}$ turns out to be −6.68 and −1.60 kcal/mol. The energies of the OH···O(H) ($E_{OH\cdots O(H)}$) and CH···O(H) ($E_{CH\cdots O(H)}$) fragments could be obtained from TT-4 and TT-6 dimers considering the following relation of binding energies.

$$E_{CH\cdots O} + E_{OH\cdots O(H)} = \Delta E^{B}(\text{TT-4}) \quad (6)$$

$$E_{CH\cdots O} + E_{CH\cdots O(H)} = \Delta E^{B}(\text{TT-6}) \quad (7)$$

Using the calculated $E_{CH\cdots O}$, the values for $E_{OH\cdots O(H)}$ and $E_{CH\cdots O(H)}$ turn out to be −3.10 and −0.82 kcal/mol respectively. With these calculated $E_{X\cdots Y}$ values and considering the *trans*- to *cis*-formic acid conversion energy (E_{TC}) to be 4.08 kcal/mol (MP2 result, Table 2s), one can calculate the binding energies of other formic acid dimers as shown below.

Dimer TT-2: $E_{TT-2} = E_{CH\cdots O} + E_{O\cdots HO} = -8.28$ kcal/mol

Dimer TC-1: $E_{TC-1} = E_{TC} + E_{CH\cdots O} + E_{O\cdots HO} = -4.20$ kcal/mol

Dimer TC-3: $E_{TC-3} = E_{TC} + E_{O\cdots HO} = -2.60$ kcal/mol

Dimer TC-4: $E_{TC-4} = E_{TC-3}$

Dimer TC-1: $E_{TC-5} = E_{TC} + E_{CH\cdots O} + E_{CH\cdots O(H)} = 1.66$ kcal/mol

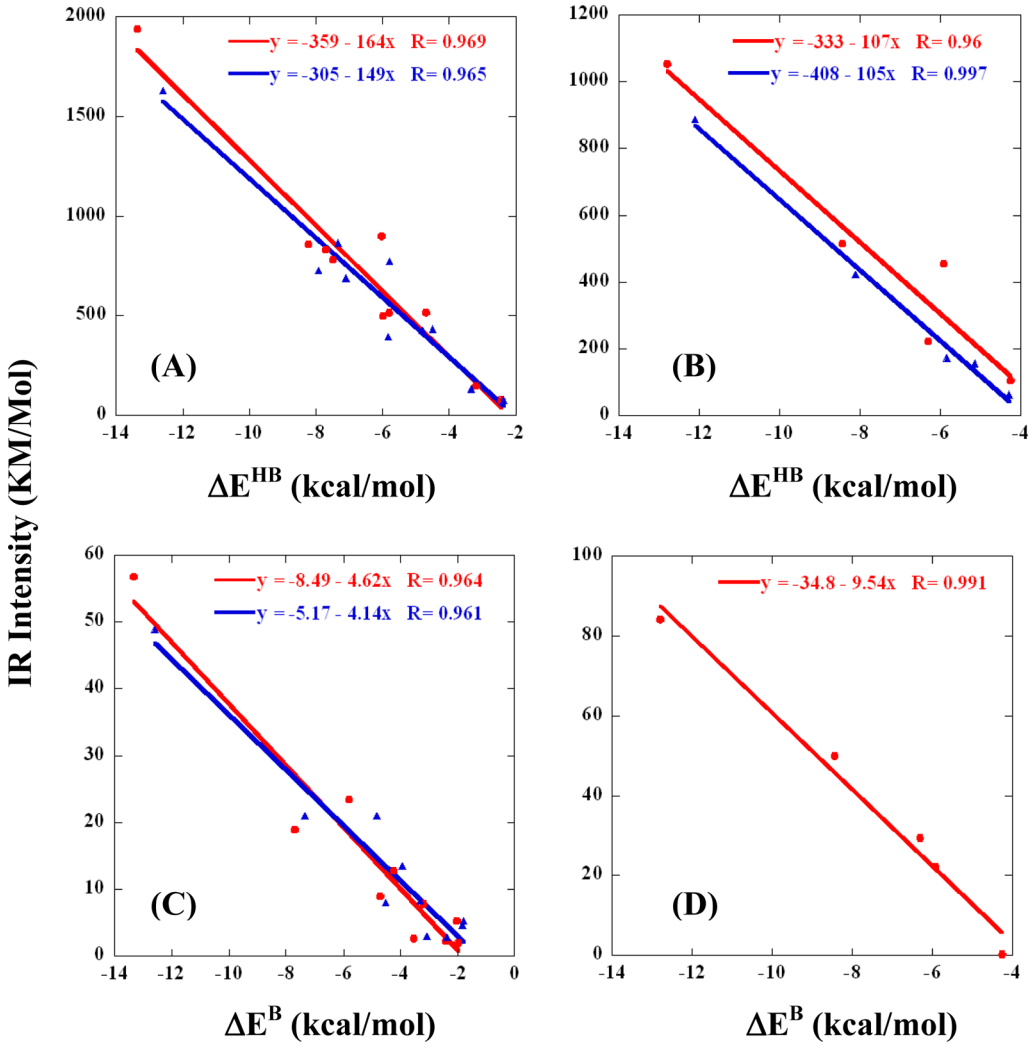

Figure 5. Correlation of IR-intensities of various formic acid and formamide dimers with their hydrogen-bond energies (ΔE^{HB})/binding energies (ΔE^{B}) is presented. Panel (a) correlation of IR-intensities of ν(OH) of various formic acid dimers (TT-1 to TC-5) against their ΔE^{HB}; panel (b) correlation of IR-intensities of ν_s(NH) of various formamide dimers (FMAD-A to FMAD-E) against their ΔE^{HB}. These IR-intensities are available in Table s3.[40] Panels (c) and (d) represent correlation of the intensities of the low-frequency in-plane bending/stretch−bend (in-plane) (depending on the structure of the dimer) of the different formic acid (c) and formamide (d) dimers against their ΔE^{B} values. The modes and the corresponding intensities are shown in Figures 1s and 2s of the Supporting Information. The red and blue lines respectively represent the MP2 and CCSD results.

These binding energy values (E-terms on the left-hand side) computed using transferable additive fragment terms are within 0.5 kcal/mol of the computed values (except TT-2, where the difference is ∼1.0 kcal/mol) presented in Table 1 and thus showing the existence of additive relation as proposed above.

In the case of formamide dimers (Figure 2), the transferable local fragments for hydrogen-bonds are NH···O and CH···O. The local binding energies for these two fragments (viz. $E_{NH\cdots O}$ and $E_{CH\cdots O}$) could be obtained from the binding energies of FMAD-A and FMAD-E dimers (Table 3, MP2 data) to be −6.43 and −2.13 kcal/mol. The binding energies of the dimers FMAD-B and FMAD-D ($E_{FMAD\text{-}B}$ and $E_{FMAD\text{-}D}$) could be computed using the following additive relations.

$$\text{Dimer FMAD-B: } E_{FMAD-B} = E_{CH\cdots O} + E_{NH\cdots O} = -8.56 \text{ kcal/mol}$$

$$\text{Dimer FMAD-D: } E_{FMAD-D} = E_{NH\cdots O} = -6.43 \text{ kcal/mol}$$

The binding energy values thus computed are very close to the respective ΔE^{B} values in Table 3. The ΔE^{B} values of both formic acid and formamide dimers at the CCSD and CCSD(T) levels are also reproduced with similar accuracy (not discussed) using the above additivity concepts. It is to be noted that the binding energies of TT-3, TC-2 (Figure 1), and FMAD-C (Figure 3) cannot be computed using such relations as the corresponding fragment values are not available from the present data. The linear correlations in Figure 5 further show, that since the binding energies of the concerned dimers have additive properties, the intensities of the frequencies involved in such correlation should also show similar additive properties.

c. Validity of the Computed Results. The validity of the correlations and the additive properties discussed above depends on the accuracy of the computed binding energies and the vibrational frequencies. It has been already shown in section III that the computed anharmonicity corrected vibrational frequencies reproduce the experimental data quite satisfactorily. Recently, a very accurate experimental estimate of the dimerization process of formic acid has been carried out by Kollipost et al.[46] using the hydrogen bond vibration fundamentals. The estimated dissociation energy (14.2 ± 0.2 kcal/mol) is very close to our computed values at the MP2 (13.35 kcal/mol) and CCSD(T) (13.23 kcal/mol) levels. We have further computed the binding energies of

dx.doi.org/10.1021/ct300889b | J. Chem. Theory Comput. 2013, 9, 1016−1026

formic acid and formamide dimers using G4MP2, G2MP2, and CBS-QB3 techniques. The methods use scale factors to compute the zero-point energies and thus indirectly include anharmonicity effect in the computed energies. The G4MP2 computations generate binding energy of TT-1 dimer (−13.14 kcal/mol) close to the MP2/au-cc-pvtz data, while the other two methods produce results (G2MP2: −12.34 kcal/mol; CBS-QB3: −12.51 kcal/mol) with somewhat lower accuracy (close to the CCSD data). Moreover, the plots of the computed ΔE^B values of formic acid and formamide dimers (Tables 6s and 7s of the Supporting Information) at the G4MP2, G2MP2, and CBS-QB3 levels against the intensities of their respective hydrogen-bond fundamentals show similar linear correlations (Figure 6), as

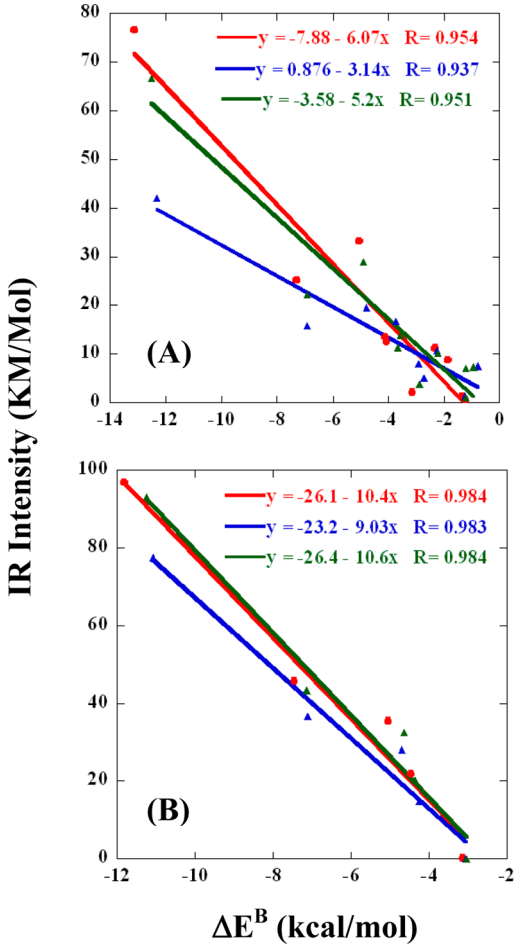

Figure 6. Correlation of the intensities of the low-frequency in-plane bending/stretch−bend (in-plane) (depending on the structure of the dimer) of the different formic acid (a) and formamide (b) dimers against their ΔE^B values at the G4MP2 (red lines), G2MP2 (blue lines), and CBS-QB3 (green lines) level of theories. The ΔE^B values, the low-frequency modes, and the corresponding IR intensities area available in Tables 6s and 7s of the Supporting Information.

observed in Figure 5. These results show that the correlations and additivity of binding energies, as observed from our results, are fully rational and unique for such dimers.

V. CONCLUSIONS

The structures of eleven formic acid and five formamide dimers were optimized at the MP2 and CCSD levels of theory to compute their binding energies and the nature of low- and high-frequency vibrational modes. The binding energies and the vibrational modes were corrected for the anharmonicity effects. The computed vibrational frequencies with anharmonicity corrections agree with the experimental data very well. The error bar is much lower than those computed without such corrections. The improvements of binding energies (ΔE^B, ΔH^B_{298}, and ΔG^B_{298}) are marginal (~0.12 to 0.15 kcal/mol change) with respect to the uncorrected data, but such improvements turn out to be quite important when thermochemistry regarding the relative stability (ΔG^B_{298}) of different dimers is analyzed. The computed binding energies of the TT-1 dimer of formic acid show good agreement with experiment and other high-accuracy energy computation techniques (viz. G4MP2, G2MP2, and CBS-QB3).

The accuracy of the computed low-frequency fundamentals (ν_i), their overtones ($[2\nu_i]$), and the mixed modes ($[\nu_i\nu_j]$) of the lowest energy formic acid dimer (TT-1) with respect to the experiment led to the further analysis of such modes for other formic acid (TT-2 to TC-5; Figure 1) and formamide (FMAD-A to FMAD-E; Figure 2) dimers. The results revealed that for both lowest energy formic acid (TT-1) and formamide (FMAD-A) dimers (C_{2h}-symmetry), the nature of their six low-frequency fundamentals is very similar and the in-plane bending and stretch−bend fundamentals of different dimers of formic acid and formamide (depending on the dimer structure) in this low-frequency region modulate the strength of hydrogen-bond/binding in such dimers and hence their relative stability order. The last observation is in conformity with the previous experiments[25,40,41] on the low-frequency modes of weakly interacting dimers. Since linear correlations exits between the intensities of the high-frequency and low-frequency modes (responsible for hydrogen-bonding) with the $\Delta E^{HB}/\Delta E^B$ of such dimers, the additive nature of binding energies (as well as intensities of the modes involved in hydrogen-bonding) of these dimers with respect to the local hydrogen-bond energies of fragments have been proposed. The additive properties are important in chemistry to explain many structural and chemical properties. Parachor is a well-known property in this respect,[47] which connects surface tension with molecular properties. Some of the more recent studies involve Lewis acidity with respect to the fluorine positions of tris-(fluorophenyl)-substituted boranes,[48] chemical element properties of binary zinc compounds,[49] and electron localization properties of hydrogen bonded compounds.[50] In several cases, these additive properties have predictive capabilities (e.g., parachor). Although, the additive nature of binding energies of the isomers of formic acid and formamide dimers seem quite natural from their investigated properties, the predictive nature of binding energies using the computed local character of the individual hydrogen bonding fragments are not tested beyond the present domain of isomers. Systematic studies on similar other systems are needed to check the transferability of the present computed parameters.

■ ASSOCIATED CONTENT

Supporting Information

Complete reference of Gaussian-09 code; Tables 1s, 2s, 3s, 4s, 5s, 6s, 7s, and Figures 1s and 2s. This material is available free of charge via the Internet at http://pubs.acs.org.

■ AUTHOR INFORMATION

Corresponding Author

*E-mail: jerzy@icnanotox.org (J.L), devashis@icnanotox.org (D.M.), szczepan.roszak@pwr.wroc.pl (S.R).

Notes

The authors declare no competing financial interest.

■ ACKNOWLEDGMENTS

This work has been supported by CREST (Award No. HRD-0833178) and EPSCOR (Award No. 362492-190200-01\NSFEPS-0903787). One of the authors (S.R.) acknowledges the financial support by a statutory activity subsidy from Polish Ministry of Science and Technology of Higher Education for the Faculty of Chemistry of Wroclaw University of Technology. We also thank the Mississippi Center for Supercomputing Research and the Wroclaw Centre for Networking and Supercomputing for providing generous computer time.

■ REFERENCES

(1) Kwei, G. H.; Curl, G. F., Jr. *J. Chem. Phys.* **1960**, *32*, 1592−1594.
(2) Winnewwisser, M.; Winnewwisser, B. P.; Stein, M.; Birk, M.; Wagner, G.; Winnewwisser, G.; Yamada, K. M. T.; Belov, S. P.; Baskakov, O. I. *J. Mol. Spectrosc.* **2002**, *216*, 259−265.
(3) Karle, J.; Brockway, L. O. *J. Am. Chem. Soc.* **1944**, *66*, 574−584.
(4) V. Shomaker, V.; O′Gorman, J. M. *J. Am. Chem. Soc.* **1947**, *69*, 2638−2644.
(5) Karle, I. L.; Karle, J. *J. Chem. Phys.* **1954**, *22*, 43−45.
(6) Millikan, R. C.; Pitzer, K. S. *J. Chem. Phys.* **1957**, *27*, 1305−1308.
(7) Tan, T. L.; Goh, K. L.; Ong, P. P.; Teo, H. H. *J. Mol. Spectrosc.* **1999**, *198*, 110−114.
(8) Bertie, J. E.; Michaelian, K. H. *J. Chem. Phys.* **1982**, *76*, 886−894.
(9) Bertie, J. E.; Michaelian, K. H.; Eysel, H. H.; Hager, D. *J. Chem. Phys.* **1986**, *85*, 4779−4789.
(10) Hocking, W. H. Y. *Z. Naturforsch.* **1976**, *31A*, 1113−1121.
(11) Pettersson, M.; Lundell, J.; Khriachtchev, L.; Räsänen, M. *J. Am. Chem. Soc.* **1997**, *119*, 11715 −11716.
(12) Roszak, S.; Gee, R. H.; Balasubramanian, K.; Fried, L. E. *J. Chem. Phys.* **2005**, *123*, 144702−1 − 144702−10.
(13) Yavuz, I. *J. Chem. Theory Comput.* **2008**, *4*, 533−541.
(14) Olbert-Majkut, A.; Ahokas, J.; Londell, J.; Petterson, M. *Chem. Phys. Lett.* **2009**, *468*, 176−183.
(15) Marushkevich, K.; Khriachtchev, L.; Lundell, J.; Domanskaya, A.; Räsänen, M. *J. Phys. Chem. A* **2010**, *114*, 3495−3502.
(16) Marushkevich, K.; Siltanen, M.; Räsänen, M.; Haloneu, L.; Khriachtchev, L. *J. Phys. Chem. Lett.* **2011**, *2*, 695−699.
(17) Marushkevich, K.; Khriachtchev, L.; Räsänen, M.; Melqvuori, M.; Londell, J. *J. Phys. Chem. A* **2012**, *116*, 2101−2108.
(18) Albrecht, M.; Rice, C. A.; Suhm, M. A. *J. Phys. Chem. A* **2008**, *112*, 7530−7542.
(19) Marrdyukov, A.; Sánchez-Garcia, E.; Rodziewicz, P.; Doltsinis, N. L.; Sander, W. *J. Phys. Chem. A* **2007**, *111*, 10552−10561.
(20) Birer, Ö.; Havenith, M. *Annu. Rev. Phys. Chem.* **2009**, *60*, 263−275.
(21) Hargis, J. C.; Vöhringer-Martinez, E.; Woodcock, H. L.; Toro-Labbé, A.; Schaefer, H. F., III *J. Phys. Chem. A* **2011**, *115*, 2650−2657.
(22) Saritha, B.; Durga Prasad, M. *J. Phys. Chem. A* **2011**, *115*, 2802−2810.
(23) Okuyama, M.; Takatsuka, K. *Bull. Chem. Soc. Jpn.* **2012**, *85*, 217−227.
(24) Grabowski, S.; Sokalski, W. A.; Leszczynski, J. *J. Phys. Chem. A* **2006**, *110*, 4772−4779.
(25) Xue, Z.; Suhm, M. A. *J. Chem. Phys.* **2009**, *131*, 054301−1−054301−4.
(26) Møller, C.; Plesset, M. *Phys. Rev.* **1943**, *46*, 618−622.
(27) Scuseria, G. E.; Janssen, C. L.; Schaefer, H. F., III *J. Chem. Phys.* **1988**, *89*, 7382−7387.
(28) McQuarrie, D. A.; Simon, D. A. *Physical Chemistry A Molecular Approach*; University Science Books: CA, 1997; Chapter 18, pp 731−755; Chapter 20, pp 840−843.
(29) Barone, V. *J. Chem. Phys.* **2004**, *120*, 3059−3065.
(30) Barone, V. *J. Chem. Phys.* **2005**, *122*, 014108−1−014108−10.
(31) Parr, R. G.; Yang, W. *Density Functional Theory of Atoms and Molecules*; Oxford: New York, 1989.
(32) Becke, A. D. *J. Chem. Phys.* **1993**, *98*, 5648−5652.
(33) Vosco, S. H.; Wilk, L.; Nusiar, M. *Can. J. Phys.* **1980**, *58*, 1200−1211.
(34) Lee, C.; Yang, W.; Parr, R. G. *Phys. Rev. B* **1988**, *37*, 785−789.
(35) Pople, J. A.; M. Head-Gordon, M.; Raghavachari, K. *J. Chem. Phys.* **1987**, *87*, 5968−5975.
(36) Curtiss, L. A.; Redfem, P. C.; Raghavachari, K. *J. Chem. Phys.* **2007**, *127*, 124105−1−124105−8.
(37) Curtiss, L. A.; Raghavachari, K.; Pople, J. A. *J. Chem. Phys.* **1993**, *98*, 1293−1298.
(38) Montgomery, J. A., Jr.; Frisch, M. J.; Ochterski, J. W.; Petersson, G. A. *J. Chem. Phys.* **2000**, *112*, 6532−6542.
(39) Frisch, M. J.; Trucks, G. W.; Schlegel, H. B. et al. computer code GAUSSIAN 09, Revision C.01; Gaussian, Inc.: Wallingford, CT, 2009.
(40) Dennington, R.; Keith, T.; Millam, J. GaussView, Version 5; Semichem Inc.: Shawnee Mission, KS, 2009.
(41) Aquino, A. J. A.; Tunega, D.; Haberhauer, G.; Gerzabek, M. H.; Lischka, H. *J. Phys. Chem. A* **2002**, *106*, 1862−1871.
(42) Full optimization of the FMAD-A geometry at the DFT/B3LYP/aug-cc-pvtz level underestimates the binding energy values by ∼1.0 kcal/mol (ΔE^{B} = −10.78 kcal/mol; ΔH^{B}_{298} = −11.24 kcal/mol; ΔG^{B}_{298} = −0.25 kcal/mol) with respect to the MP2 results at the same level (see Table 3).
(43) Herzberg, G. *Molecular Spectra and Molecular Structure. II. Infrared and Raman Spectra of Polyatomic Molecules*; Van Nostrand: Princeton, 1945.
(44) Heyne, K.; Huse, N.; Dreyer, J.; Nibbering, E. T. J.; Elsaesser, T.; Mukamel, S. *J. Chem. Phys.* **2004**, *121*, 902−913.
(45) Petersen, P. B.; Roberts, S. T.; Ramasesha, K.; Nocera, D. G.; Tokmakoff, A. *J. Phys. Chem. B* **2008**, *112*, 13167−13171.
(46) Kollipost, F.; Larsen, R. W.; Domanskaya, A. V.; Nörenberg, M.; Shum, M. A. *J. Chem. Phys.* **2012**, *136*, 151101−1−151101−4.
(47) Exner, O. *Nature* **1962**, *196*, 890−891.
(48) Durfey, B. L.; Gilbert, T. M. *Inorg. Chem.* **2011**, *50*, 7871−7879.
(49) Wu, P.; Jin, H. M.; Li, Y. *Chem. Mater.* **1999**, *11*, 3166−3170.
(50) Navarrete-López, A. M.; Garza, J.; Vargas, R. *J. Phys. Chem. A* **2007**, *111*, 11147−11152.